Mansoura Engineering Journal

Volume 25 | Issue 1 Article 7

2-4-2021

Vibration and Noise due to the Interaction between Fluid and a Variable Speed Hermetic Reciprocating Compressor.

N. Mostafa
Mechanical Power Engineering Department., Faculty of Engineering., Zagazig University., Zagazig., Egypt.,
nmostafa@ut.edu

Vibration And Noise due to The Interaction Between Fluid And A Variable Speed Hermetic Reciprocating Compressor

الإهتزازات و الضوضاء الناتجة عن التأثير المتبادل بين المائع و ضاغط ترددى مقفل متغير السرعه

by

N. H. Mostafa*
Visiting Prof. ESM Department
VIRGINIA POLYTECHNIC INSTITUTE AND STATE UNIVERSITY
Blacksburg, VA 24061-0219
E-mail: nmostafa@vt.edu

خلاصه:

أن توفير الطاقة مع تقليل الضوضاء و الإهتزازات لمن أهم الاهداف فى أجهزه التبريد و التكييف. لقد استعمل ضاغط ترددى صغير و غيرت سرعته بدلا من إستعمال نظام التحكم فى الحمل الحرارى عن طريق الإيقاف و التشغيل نسبه للحمل الحرارى. و بناء على ذلك فانه لمن المهم دراسة الضوضاء و الإهتزازات الناتجه عن أحمال و سرعات مختلفة و الناتجه عن سريان المائع بداخلة.

أحد الأسباب فى اثاره اهتزازات جسم ضاغط التبريد الترددى المغلق هو التغير الدورى فى ضغط الغاز وتأثير ذلك علي أجزاء الضاغط المختلفة. هذا التغير فى الضغط نتيجة غلق وفتح صمامات السحب و الطرد. أن تاثير عدم الإتزان فى الضغوط يؤدى الى هز جسم الضاغط الذى يؤثر بالتالى بقوى مختلفة على حمالات الضاغط مع الغلاف الخارجى للضاغط المقفل. و نتيجة لذلك فان الغلاف الخارجى يشع موجات من الضوضاء المختلفة.

ان ترددات الضوضاء و الإهتزازات الناتجة عن سريان المائع وجد انها دالة فى سرعة دوران الضاغط. ان ترددات الإثاره للضاغط فى مستوى الضوضاء وجد انها متوافقة مع ١٢, ١٦, ٢٠, ٣٠, ٣٢, ٤١, ٧٥ مرة مماثلة لسرعة دوران الضاغط. ان ترددات الإثاره للضاغط فى مستوى إهتزازات العجلة و التى تتاثر بديناميكا حركه الغازات داخل الضاغط وجد انها متوافقة مع ١٢, ٢٢, ٢٦, ٤١, ٧٥ مرة مماثلة لسرعة دوران الضاغط.

ان إسلوب التحكم فى الحمل الحرارى فى الضاغط الترددى المغلق باسلوب التحكم فى السرعة بدلا من النظم المعتاد بالتشغيل و الإيقاف اعطى مجال واسع للاداء بمستوى منخفض من الضوضاء و الإهتزازات.

---

* Associate Prof. Mechanical Depart., Zagazig university, Egypt.

Accepted February 7, 2000

ABSTRACT:

Energy saving with minimum of noise and vibration levels has been very important tasks, specially, in the refrigeration and air conditioning field. Variable speed reciprocating compressor is used in small residential unit to control the load capacity instead of on/off control. Based on this, it is important to study the noise and vibration generated at different compressor loads, speed and fluid flow parameters.

One of the causes of excitation of the housing of the hermetic compressors in commercial refrigeration is the periodic gas pressure variation, which interact with many compressor elements. These variations are mainly due to the opening and closing movement of the suction and exhaust valves. Unbalanced pressure effects cause shaking of the compressor which, in turn, cause compressor suspension forces to excite the compressor shell. The compressor shell then radiates acoustic noise.

The noise and vibration generated from fluid flow are found function of compressor speed. The excitation frequencies seen in sound pressure response that are most influenced by the fluid dynamics are 12, 16, 20, 30, 32, 41, 75 times of the running speed. Also, the vibration frequencies that dominate the acceleration level and that are affected by the aerothermodynamic parameters on the compressor levels are 12, 22, 26, 41, 75 times of running speed.

This speed control gives a wide range of capacity load control operation with decreasing sound and vibration level, which is much lower than on/off control.

NOMENCLATURE:

a : Vibration acceleration level on casing (m/s^2).
I_s : Near-field sound intensity (dB).
n : Rotor speed (rps).
r : Pressure ratio (P_{s2}/P_{s1})
P_1 : pressure of fluid at compressor inlet (Pa).
P_2 :Pressure of fluid at compressor outlet (Pa).
P_{DB}: Dynamic pressure at bottom of cylinder (Pa).
P_{Dh} :Dynamic pressure at housing cavity (Pa).
P_{DT} :Dynamic pressure at top of cylinder (Pa).
T : Temperature. (C°)

Subscript:

1 : Compressor inlet / suction.
2 : Compressor outlet / exhaust.
S : Static.
D : Dynamic.

INTRODUCTION:

Most large machines of turbomachinery use a variable speed system to control the load capacity, specially in refrigeration and air conditioning field. Such systems have many advantages in controlling the load with minimum excitation of vibration (Mostafa 1994-1).These systems have the ability to optimize the operating parameters with load as has been done in steam turbines and centrifugal compressors (Mostafa 1994-2). In the area of residential air-conditioners and household refrigerators, on/off control is commonly used as a capacity control. This (on/off) technique is cheaper and simple to implement. However, It's disadvantage is an unavoidable reduction of Seasonal Energy Efficiency Ratio (SEER) due to the on/off cycling losse [Liu and Soedel 1994-1]. Also, room temperature will not be stable due to (on/off) control system. The compressor efficiency and discharge gas pulsation of a variable speed compressor are discussed by Liu and Soedel (1994-2). Using Helmholtz resonator model and compared the results experimentally.

The following research is part of a series of studies to more fully understand sound propagation from hermetic reciprocating compressors. The sound levels emitted from the

operation of the reciprocating compressor were studied by Craun (1994). Compressor assembly modeling by Ramani et al. (1994) involves detailed solid modeling of internal component for inertia properties, developing reduced-degree-of-freedom finite element models of the mounting springs, modeling of shockloop and modeling of the sealed external shell. Eighty seven natural frequencies below 2000 Hz (excluding the rigid-body modes) were found using the finite-element-based compressor assembly model. This model can be used to predict velocity responses on the surface of the sealed shell. These velocities are used in sound emission predictions.

Experimental model testing was performed by Rose (1994) using impact testing to determine the compressor frequency response functions. Twenty three natural frequencies were identified for the compressor housing in the frequency range below 2000 Hz. These were correlated and the Finitc Element Model updated by Ramani et al.(1994).

Through the use of multiple-input /single-output (MISO) modeling, the propagation paths of sound within a reciprocating hermetic compressor have been investigated and ranked by Craun (1994). Using compressor far-field sound output, suspension spring forces, and internal suction, exhaust, and housing pressure fluctuations, a MISO model has been developed. This model identified the importance of the suspension system forces in generating the compressor far-field sound spectrum.

Furthermore, the compressor's vibrations change with different operation conditions as discussed by Mostafa (1994) in an industrial centrifugal compressor. The aerothermodynamic parameters such as output-to-input pressure ratio and rotor speed have an influence upon vibration level. This relation can be described by a second-degree polynomial. Aerothermodynamic vibrations is synchronized with the fluid blade interaction frequencies in centrifugal compressor.

The aim of the current work is to determine the vibration and acoustic signature for a range of compressor performances. These performances are concerned with the influence of the thermodynamic parameters such as pressure, pressure ratio and (suction, discharge, evaporator inlet and condenser outlet) temperatures on the noise and vibration levels. These thermodynamic parameters are thought to influence the structureborne vibrations that have been shown to directly dominant the noise emission. This will be done while the compressor is working under different speeds that have an effect upon the compressor load, vibration and sound level.

COMPRESSOR TEST SETUP:

The test loop was built and installed at the Virginia Polytechnic Institute and State University, Mechanical Engineering Department. The compressor is a two-cylinder, reciprocating, hermetically sealed refrigeration compressor used in commercial settings.

The volumetric efficiency of the compressor is 79.8%. This efficieney was ealculated by the manufacturer using the ARI (American Refrigeration Institute) rating condition (45°F evaporator, 20°F superheat, 130°F condenser, 15°F subcooling, 95°F ambient) and assumes a running speed of 3500 rpm. The version studied here is driven by a 4.92 hp(3730w), squirrel-eage, three-phase, AC electric motor. The compressor was set on its standard rubber mounting grommets and placed on hard concrete. The compressor / test bench system was charged with R-22 refrigerant . The motor of the compressor is controlled by a variable speed system using a frequency-control technique. The nominal speed of the compressor motor is 57.8 rps.

EXPERIMENTAL INSTRUMENTATION:

To discuss the aerothermodynamic parameters that affect vibration and noise, it was necessary to collect spectral data from a compressor operating under different conditions. Thus, it is neeessary to install instrumentation inside the compressor housing as shown in Fig. (1).

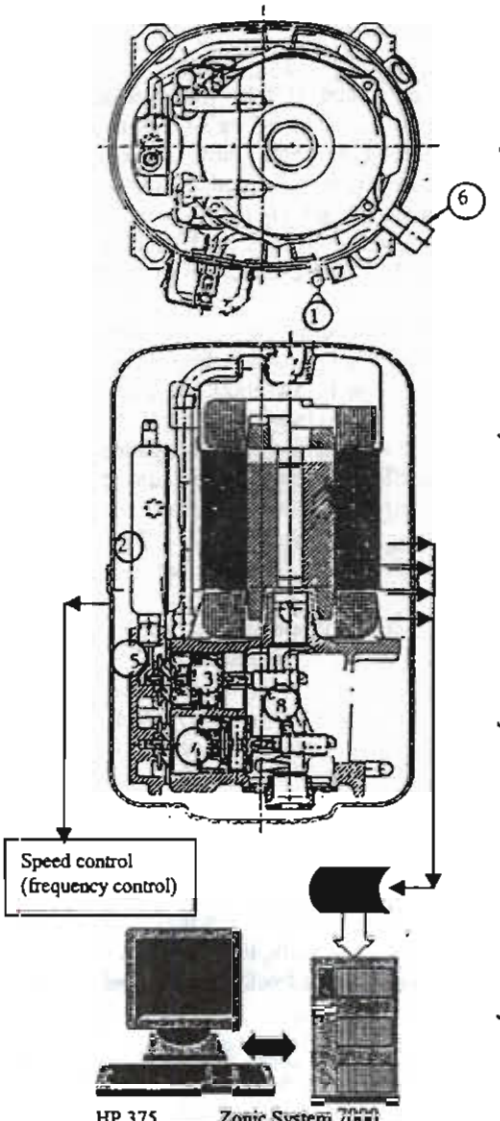

1	Sound level near field microphone
2	Housing pressure transducer
3	Top cylinder pressure transducer
4	Bottom pressure transducer
5	Exhaust pressure transducer
6	Suction pressure transducer
7	Vibration accelerometer
8	Crankshaft gear

Fig. (1) Instrumentation of The compressor

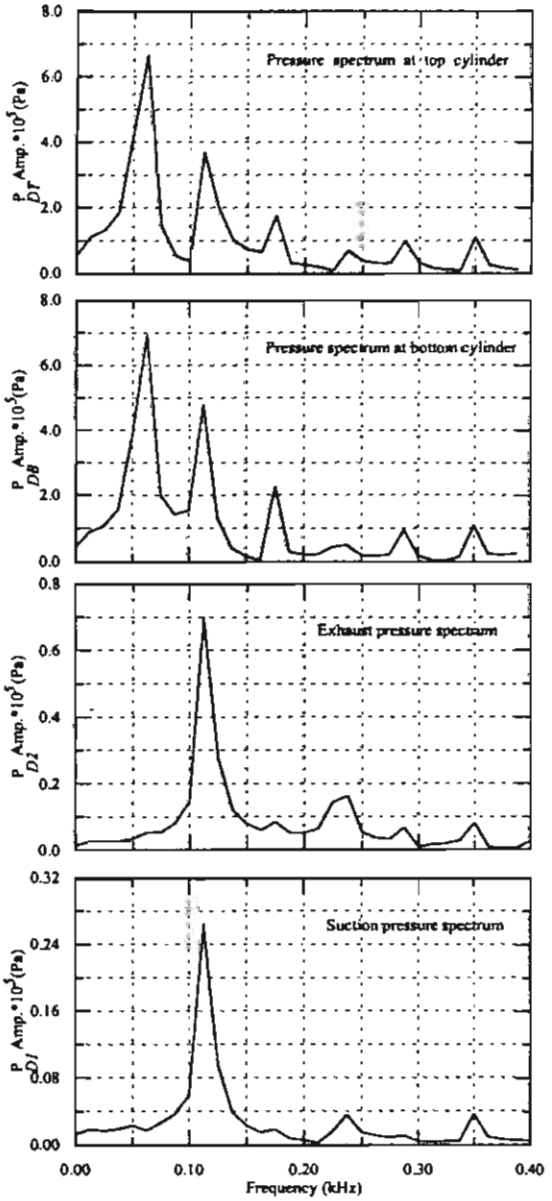

Fig. (2) Dynamic pressure spectrum of P_{DT}, P_{DB}, P_{D2} and P_{D1} at (P_{LS}= 4.86x10^5 & P_{Ds}=19.44x10^5 & n=57.8 rps).

To measure the pressure fluctuation which might drive the shell vibration, five piezoelectric pressure transducers were placed inside the compressor. One within the compressor shell cavity, one near the compressor suction line and one within the compressor exhaust line. The other two pressure transducers were placed in the compressor top and bottom cylinder. Shell vibration and near-field sound were also measured with a piezoelectric sensor and a microphone, respectively.

As can be seen in Fig.(1), the instrumentation were routed to their appropriate signal conditioning amplifiers and then into a Zonic System 7000 data acquisition unit. This unit was then connected via Ethernet to a Hewlett-Packard HP375 workstation running Zonic Zeta (Ver. 4.22) software to control the System 7000. A magnetic pickup sensed a gear on the crankshaft to reference the signals to the compression process. This gear (72 teeth) had one tooth removed to indicate the top dead center of the piston motion. For each test, 5 consecutive data blocks were acquired simultaneously from the microphone, pressure transducers, and other instrumentation. Data blocks were 1024 data points long, with sampling rate of 0.0781 ms/sample. This resulted in a spectral resolution of 12.5 Hz and baseband analysis frequencies up to 5000 Hz. Fast response thermocouples type (T) were installed at compressor inlet and outlet, and at the expansion valve inlet and outlet. The static pressure at compressor inlet and outlet was measured.

RESULTS:

The acoustic and vibration response of the compressor are caused by the periodic variation of the gas pressures in the compressor system. These are mainly due to the opening and closing movements of the suction and exhaust valves which generate a pressure field on the internal surfaces of the valves themselves. For this reason Fig. (2) shows the spectrum of the internal pressure in the top and bottom cylinders, the exhaust pressure, and the suction pressure, respectively. The pressure spectrum for top and bottom of cylinder are similar. The main peaks appear at the running speed and its harmonics, especially, the second and the third. But, in the exhaust pressure and suction pressure the first and the third harmonics of running speed disappear completely. This is caused by the two pistons being exactly 180 degrees out of phase. The base frequency in the suction and exhaust is twice the running speed. The peak of the second harmonic of running speed in the exhaust and suction is reduced to 1/10 and 1/27 of the cylinder pressures at one time running speed, respectively.

Figure (3) shows the dynamic pressure of bottom cylinder (P_{DB}) as a linear function of the dynamic pressure of top cylinder (P_{DT}) at 112.5 Hz. Dynamic suction and exhaust pressures of the compressor (P_{D1},P_{D2}) at 112.5 Hz increase in polynomial form with increasing P_{DT}. The sound pressure inside the housing cavity (P_{Dh}) at 112.5 Hz increases with increasing P_{DT}, with higher magnitude.

Figures (4) & (5) represent the sound pressure spectrum inside and outside the compressor housing, respectively. The peaks shown are the harmonics of the 57.8 rps running speed. The compressor excitation is caused by the periodic action of the pistons and valves system. These actions cause a rich harmonic complement of forces. When a particular harmonic component approaches a system resonance frequency one expects an increase in compressor vibration and/or sound. From these figures and other operating conditions the following peaks appear to be a strongly function of the operating condition; 700, 912.5, 1162.5, 1737.5, 1862.5, 2387.5, and 4337.5 Hz. Of course, other peaks appear in these figures. They remain substantially steady with load variation. Peaks 1, 2, 3 and 5 are resonance frequencies of the assembled compressor as demonstrated by Rose (1994). The fourth peak is between all known system resonance. Thus, here these variation of sound pressure with load can be attributed solely to forcing function variations.

By following the amplitudes at these frequencies for various operating conditions, one will develop different response surfaces shown in Fig.(6). These figures show the sound pressure level as a function of the static suction and exhaust pressures. Note that the overall

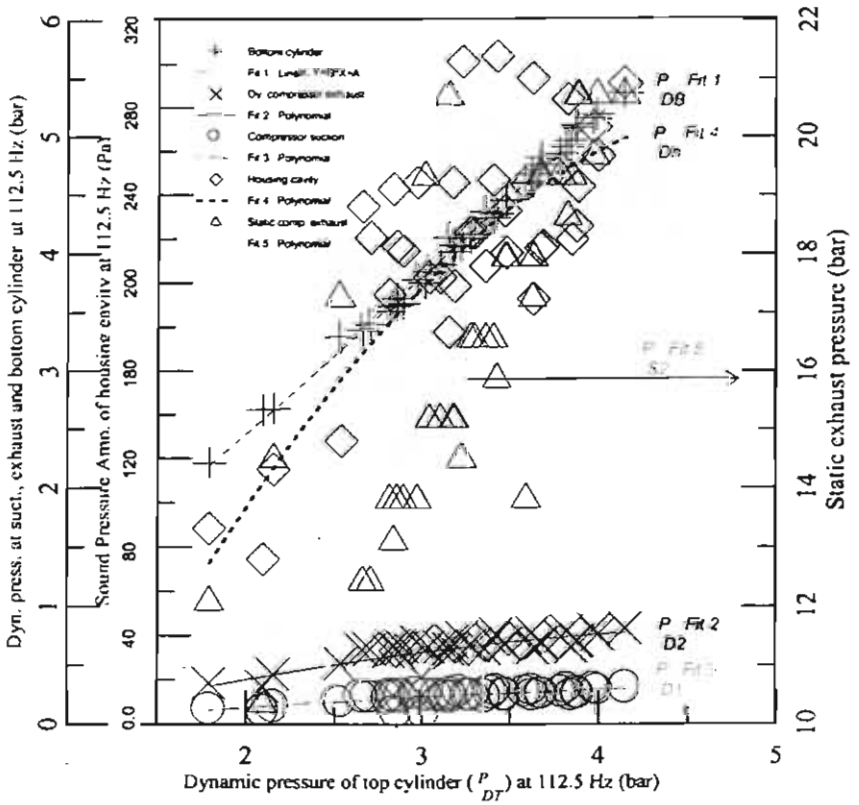

Fig. (3) Compressor performance for dynamic pressure at 112.5 Hz (speed n =57.8 rps)

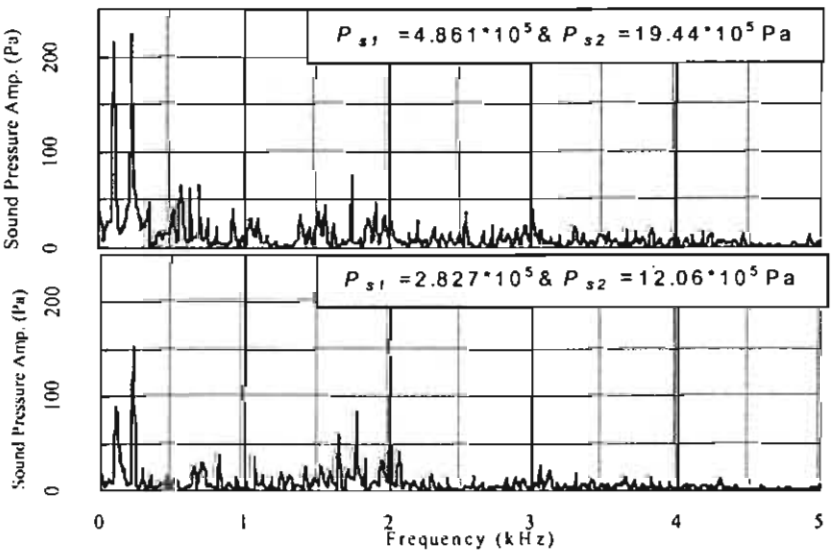

Fig. (4) Sound spectrun inside the housing cavity at different conditions. (n=57.8 rps).

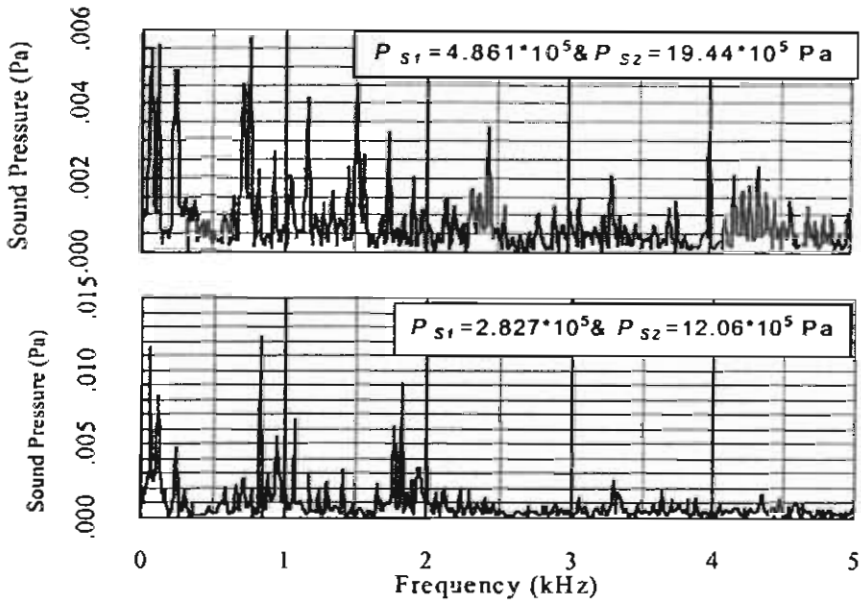

Fig. (5) Sound spectrum outside the compressor at different conditions. (n=57.8 rps).

sound pressure level has a relation increasing along the diagonal from minimum to maximum suction and exhaust pressures. This relation and all the following are highly significant with second degree form. This analytically is:

$$I_s(\textit{Overall sound}) = 96.86 - 3.732\,(P_{S1}\times10^{-5}) + 1.698(P_{S2}\times10^{-5}) + 0.2094(P_{S1}\times10^{-5})^2 + 0.1184(P_{S1}P_{S2}\times10^{-25}) \quad (1)$$

Figure (6) shows also that the first three frequencies (700, 912.5 and 1162.5 Hz) have the maximum peaks at maximum exhaust pressure with suction pressure around 4.2×10^5 Pa. These equations are discribed as:

$$I_{s(\text{at } 700\text{ Hz})} = 22.195 + 12.58\,(P_{S1}\times10^{-5}) - 1.29(P_{S1}\times10^{-5})^2 - 0.0177(P_{S2}\times10^{-5})^2 \quad (2)$$

$$I_{s(\text{at } 912.5\text{ Hz})} = 6.5 + 15.09\,(P_{S1}\times10^{-5}) - 1.996(P_{S1}\times10^{-5})^2 + 0.144(P_{S1}P_{S2}\times10^{-25}) \quad (3)$$

$$I_{s(\text{at } 1162.5\text{ Hz})} = 16.31 - 15.5\,(P_{S1}\times10^{-5}) - 1.63(P_{S1}\times10^{-5})^2 - 0.0144(P_{S2}\times10^{-5})^2 \quad (4)$$

At 1737.5 and 1862.5 Hz other important peaks appear at exhaust pressure around 14.5×10^5 Pa with suction pressure equal to 3.4×10^5 Pa. The higher exhaust and suction pressure result in lower noise level. These relation are:

$$I_{s(\text{at } 1737.5\text{ Hz})} = 24.514 + 0.185(P_{S1}P_{S2}\times10^{-25}) \quad (5)$$

$$I_{s(\text{at } 1862.5\text{ Hz})} = 8.811 + 16.639(P_{S1}\times10^{-5}) - 1.969(P_{S1}\times10^{-5})^2 \quad (6)$$

At 2387.5 and 4337.5 Hz the peaks increase at higher suction and exhaust pressure according to the following equations:

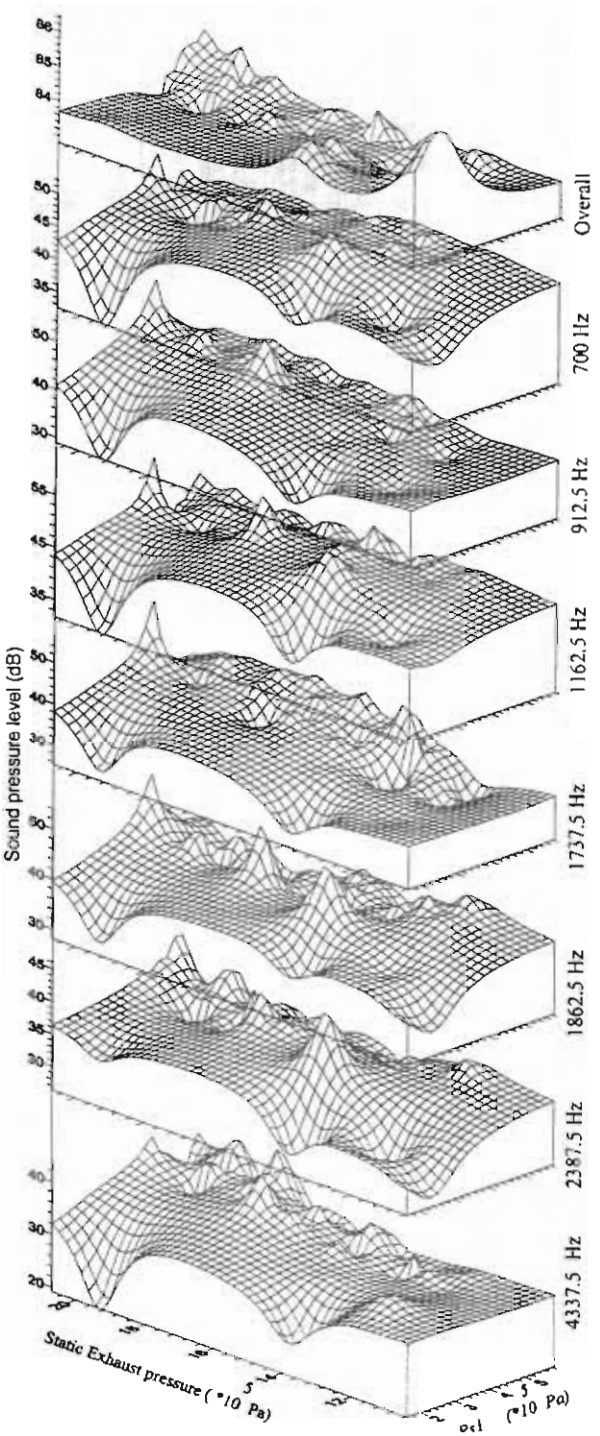

Fig. (6) Sound spectrum function of static pressure at exhaust and suction of compressor (n =57.8 rps).

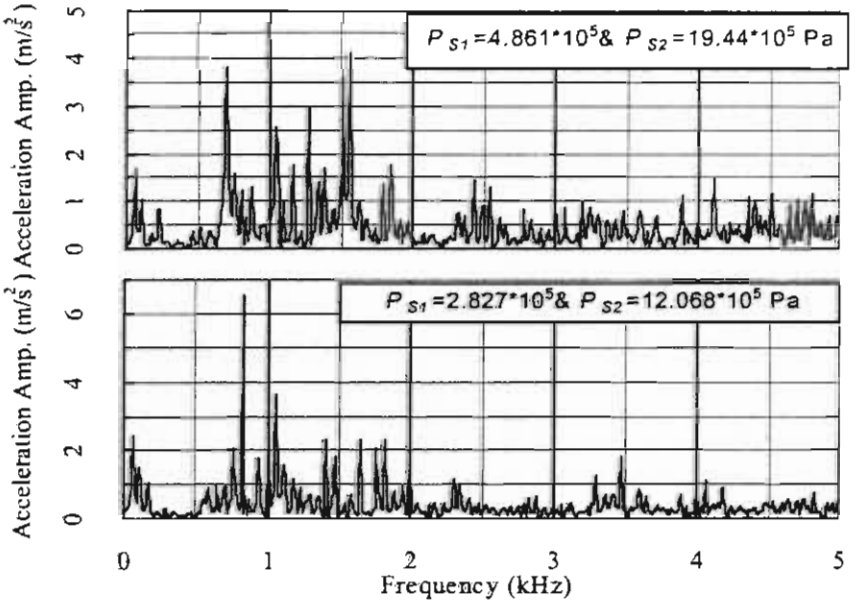

Fig. (7) Vibration spectrum at compressor casing, (n =57.8 rps)

$$I_{s(at\ 2387.5\ Hz)} = 2.877+17.351(P_{S1}\text{x}10^{-5})-2.072(P_{S1}\text{x}10^{-5})^2 \quad (7)$$

$$I_{s(at\ 4337.5\ Hz)} = 50.44-2.68(P_{S2}\text{x}10^{-5})-1.26(P_{S1}\text{x}10^{-5})^2+0.1184(P_{S1}P_{S2}\text{x}10^{-25}) \quad (8)$$

Figure (7) represents the vibration spectrum at the long face of the compressor, Fig. (1), which is recommended to pickup most of the radiated frequencies by Craun (1994). From this figure and other operating conditions, the peaks that change significantly with load, were 700, 1275, 1512.5, 1962.5 and 4750 Hz. The first and the fourth one are matched with compressor resonances. By following the amplitudes at these frequencies for various operating conditions, one can develop the response surfaces shown in Fig. (8). These figures show the acceleration level as a function of the static suction and exhaust pressures. The response surface at 700 and 1275 Hz have the same trends. In both cases the acceleration peaks are at an exhaust pressure of $14.5\text{x}10^5$ Pa and maximum suction pressure $6.25\text{x}10^5$ Pa. These relations are:

$$a_{(at\ 700\ Hz)} = -12+1.698(P_{S2}\text{x}10^{-5})+0.33(P_{S1}\text{x}10^{-5})^2 -0.0463(P_{S2}\text{x}10^{-5})^2 -0.0897(P_{S1}P_{S2}\text{x}10^{-25}) \quad (9)$$

$$a_{(at\ 1275\ Hz)} = -2.58+1.658(P_{S1}\text{x}10^{-5})-0.032(P_{S1}P_{S2}\text{x}10^{-25}) \quad (10)$$

The response surface of 1512.5 Hz, 1962.5 Hz, and the 4750 Hz acceleration appear to have the same trend, but with many more peaks along the $5.8\text{x}10^5$ Pa suction line. The following equations apply:

$$a_{(at\ 1512.5\ Hz)} = -1.071-0.0069(P_{S2}\text{x}10^{-5})^2+0.09(P_{S1}P_{S2}\text{x}10^{-25}) \quad (11)$$

$$a_{(at\ 1962.5\ Hz)} = 5.385-2.658(P_{S1}\text{x}10^{-5})+0.208(P_{S1}\text{x}10^{-5})^2 -0.00697(P_{S2}\text{x}10^{-5})^2+0.0656(P_{S1}P_{S2}\text{x}10^{-25}) \quad (12)$$

The response surface of 4750 Hz has the same trend with maximum peaks occur along a line of suction pressure equal about $4.4\text{x}10^5$ Pa and starting at exhaust pressures of $12\text{x}10^5$ Pa with the following equations:

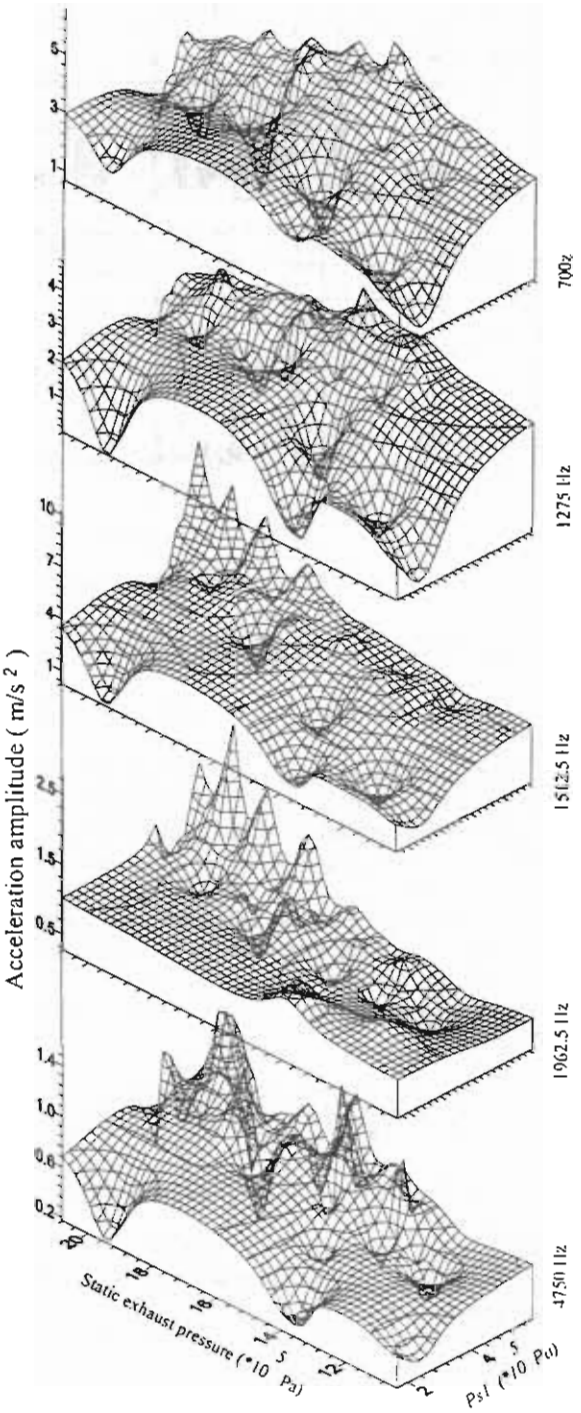

Fig. (8) Vibration spectrum function of exhaust and suction pressure (n =57.8 rps).

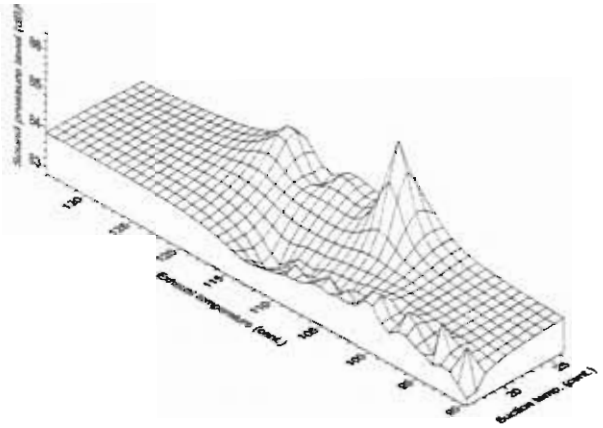

Fig. (9) sound pressure level function of suction and exhaust temperatures (n = 57.8 rps)

$$a_{(at\ 4750\ Hz)} = 0.07179 + 0.008461(P_{S1}\ P_{S2}x10^{-25}) \quad (13)$$

All the above relations are significant within the tested operating range (P_{S1}=(1.6 to 5.9) x10^5 Pa & P_{S2}=(10.4 to 20.8) x10^5 Pa).

Figure (9) represents the sound pressure level as a function of the suction and exhaust compressor temperature. This figure shows that maximum sound pressure level appears around (105-120 C° exhaust) with suction temperature between 23-25 C°. This figure gives a complete indication that the capacity load control will give a wide range of operation with low sound intensity level.

Using the speed control system, the compressor system gives a wide range of operating pressure ratio from 2.07 - 7.6. Using these operating conditions at different frequencies and running speeds, one can develop the different response surfaces shown in Fig. (10). These figures show the sound pressure level as a function of pressure ratio and running speed. Note that the overall sound pressure level has an increasing relation along the minimum pressure ratio line with increasing running speed. This relation:

$$I_s(Overall\ sound) = 60.7157 + 0.5893xn - 0.00464xn^2 - 0.1938xr^2 + 0.0357xnxr \quad (14)$$

Figure (10) shows also that the three frequencies (12xn, 20xn and 30xn Hz) have the maximum peaks at minimum pressure ratio with maximum and minimum running speeds. These relations are:

$$I_{st\ at\ 12xn\ Hz} = 44 + 0.2225xn - 3.1504xr \quad (15)$$

$$I_{stat\ 20xn\ Hz} = -24.32 + 2.8161xn - 3.444xr - 0.0242xn^2 \quad (16)$$

$$I_{st\ at\ 30xn\ Hz} = 32.5887 - 0.7421xr^2 + 0.0864xnxr \quad (17)$$

At 16xn Hz other important peaks appear at a lower speed, around 64 rps, with minimum pressure ratio (around 3). This relation is:

$$I_{stat\ 16xn\ Hz} = 35.82 - 0.7607xr^2 + 0.0804xnxr \quad (18)$$

At 32xn, 41xn and 75xn the peaks increase at higher speed (from 54xn to 70xn) and minimum pressure ratio with the following equations:

$$I_{s(at\ 32xn\ Hz)} = 34.623 - 0.6952xr^2 + 0.091xnxr \quad (19)$$

$$I_{s(at\ 41xn\ Hz)} = 30.498 - 0.5774xr^2 + 0.755xnxr \quad (20)$$

$$I_{s(at\ 75xn\ Hz)} = 34.3443 - 0.0066xn^2 - 1.635xr^2 + 0.222xnxr \quad (21)$$

The vibration frequencies dominating the acceleration level that are affected by the pressure ratio and running speed are 12, 22, 26, 41, 75 times of the running speed. Figure (11) shows the first three frequencies (12xn, 22xn, 26xn Hz) have the maximum peaks at the minimum pressure ratio and motor speed of 54 rps. These relations are:

$$a_{(at\ 12xn\ Hz)} = -4.0006 + 0.5466xn - 3.8887xr - 0.0045xn^2 + 0.3345xr^2 \quad (22)$$

$$a_{(at\ 22xn\ Hz)} = -15.352 + 0.6501xn - 0.0041xn^2 + 0.191183xr^2 - 0.0438xnxr \quad (23)$$

$$a_{(at\ 26xn\ Hz)} = -27.31 + 1.1188xn - 0.0093xn^2 - 0.0146xnxr \quad (24)$$

At 41xn and 75xn Hz other important peaks appear at lower pressure ratio around 2.1 and 3 with running speeds equal to 70 and 62 rps respectively. These relations are:

$$a_{(at\ 41xn\ Hz)} = 0.0608 - 0.0451r^2 + 0.0065\ n.r \quad (25)$$

$$a_{(at\ 75xn\ Hz)} = 0.0466 - 0.0301\ r^2 + 0.00435\ n.r \quad (26)$$

It is clear that the vibration acceleration is function of running speed with minimum level at minimum speed.

Figure (12) presents the external overall sound pressure level as a function of compression ratio and acceleration level. This figure shows that maximum sound pressure level appears from 4.7 to 5 compression ratio with maximum acceleration. The minimum SPL occurs at minimum pressure ratio.

CONCLUSION:

One of the causes of excitation of the housing of the hermetic reciprocating refrigeration compressors is the periodic gas pressure variations which interact with many compressor elements.

* The sound pressure level inside the housing cavity have higher values at the highest dynamic pressure of bottom and top of cylinder with frequency equal to the running speed multiplied by the number of 180 degrees out of phase cylinders. The same trend is seen with dynamic suction and exhaust pressures.
* The main frequencies of sound pressure level that affected by the aerothermodynamic parameters are 712.5 Hz, 912.5 Hz, 1162.5 Hz, 1737.5 Hz, 1862.5 Hz, 2387.5 Hz and 4337.5 Hz at a speed of 57.8 rps. These peaks maintained significance at 12xn, 16xn, 20xn, 30xn, 32xn, 41xn, 75xn Hz over varying the running speed (from 35 to 72 rps). The first three and the fifth are matched with the compressor resonances.
* The main frequencies of acceleration level that are affected by the aerothermodynamic parameters are 700 Hz, 1275 Hz, 1512.5 Hz, 1962.5 Hz and 4750 Hz at a running speed equal 57.8 rps.
* By varying the compressor speed (from 35 to 72 rps) the corresponding frequencies of acceleration level that are affected by the aerothermodynamic parameters are 12 rps, 22

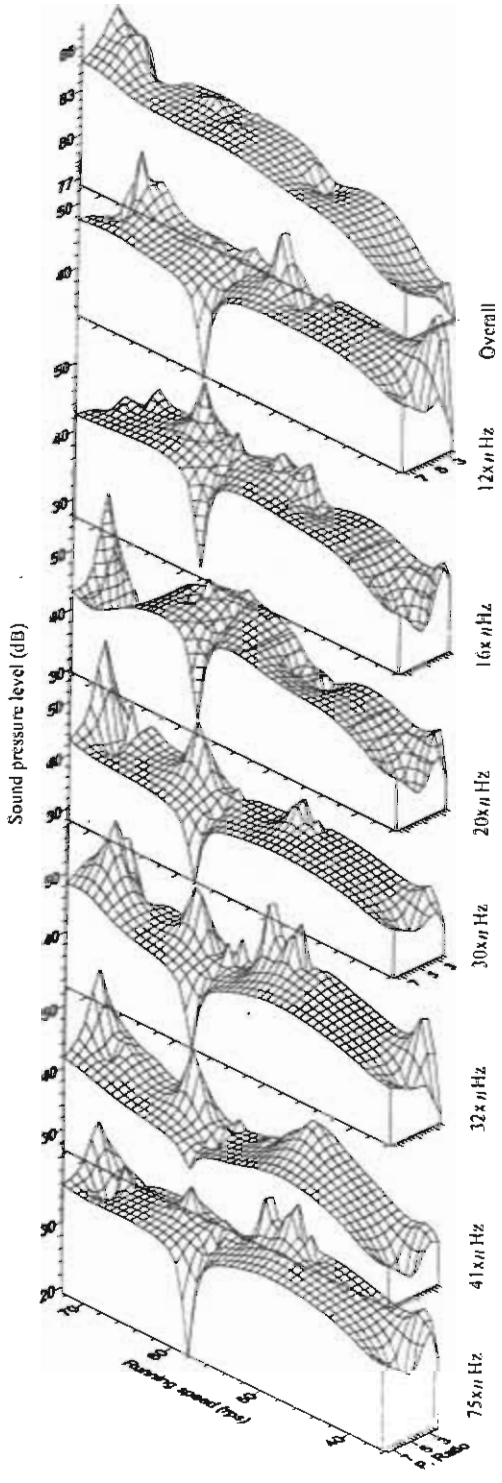

Fig. (10) Sound spectrum function of running speed and pressure ratio.

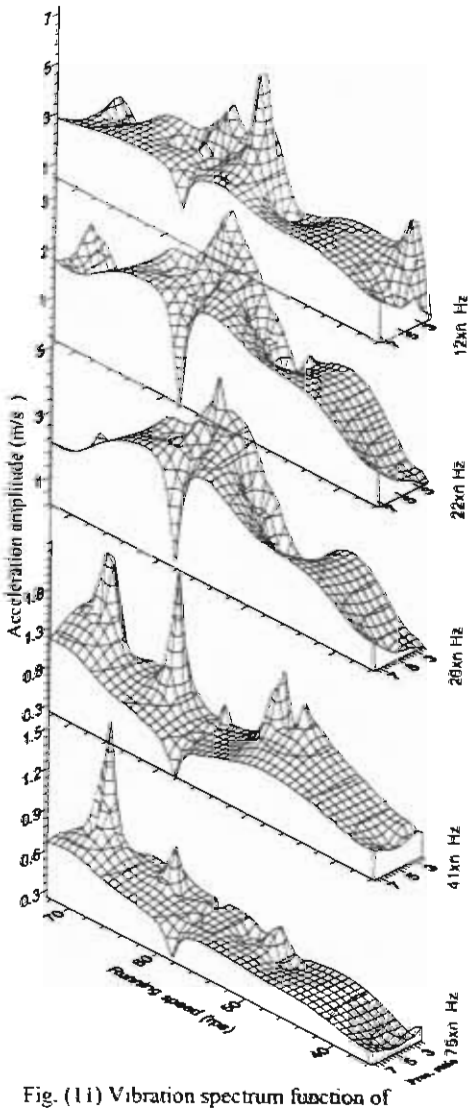

Fig. (11) Vibration spectrum function of running speed and pressure ratio.

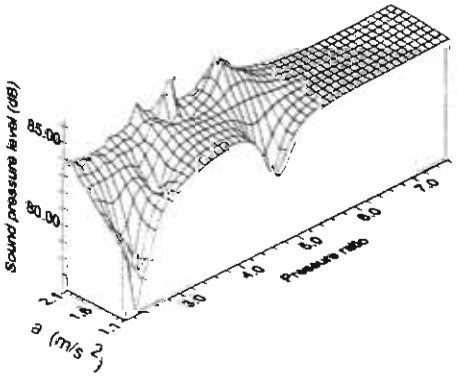

Fig. (12) Overall sound pressure level function of pressure ratio and overall acceleration of vibration.

rps and 26 rps which are matched with the compressor resonances. But, with varying the speed the harmonic 41 and 75 of the running speed have also significant relation with pressure ratio and running speed.

* The sound pressure level and vibration at these corresponding frequencies have significant second degree relations function of pressure suction and exhaust of the compressor or with pressure ratio and running speed.
* The maximum sound pressure level appears around (105-120 C°) with higher compressor suction temperature and at compression ratio 4.7 to 5.
* A wide range of operation is available using the speed control system which also, at a lower speed (lower load) emitted lower noise level and vibration intensity.

This data could be useful for using speed control instead of (on/off) system for saving energy with wide operation range, lower vibration and sound levels.

In the future this data could provide a knowledge base for an expert system which would enable to spot instantaneously the parameters which are affecting the compressor performance.

REFERENCES:

Craun, M. A., 1994, "*Identification of Sound Transmission Paths within a Hermetic Reciprocating Refrigeration Compressor Via Multiple-Input/ Single-Output Modeling*" M. Sc. Thesis, Virginia Polytechnic Institute and State University, Mechanical Eng. Department, Blacksburg, VA, U.S.A.

Liu Zheji and Soedel Werner, 1994, "Performance Study of A Variable Speed Compressor With Special Attention to Supercharging Effect" *Proceeding of International Compressor Engineering Conference at Purdue*, Purdue University, West Lafayette, Indiana, USA. PP 499-506.

Liu Zheji and Soedel Werner, 1994, " Discharge Gas Pulsations In A Variable Speed Compressor" *Proceeding of International Compressor Engineering Conference at Purdue,* Purdue University, West Lafayette, Indiana, USA. pp. 507-514.

Mostafa, N. H., 1994, "Aerothermodynamic Vibration Correlation in an Industrial Compressor Turbine Unit", *Proceeding of ASME The Fluids Engineering Division Summer Meeting,* Fluid Maehinery Forum, Nevada, U.S.A., FED Vol. 195. PP. 35-41.

Mostafa, N. H., 1994, "Steam Distribution Excitation Between High & Medium Pressure Turbines" *Proceeding of ASME The Fluids Engineering Division Summer Meeting,* FED, Fluid Machinery Forum, Nevada, U.S.A., Vol. 195. PP. 19-23.

Ramani, A., Rose, J., Knight, C. E. and Mitchell, L. D., 1994, "Finite Element Modeling of a Compressor For Sound Prediction Purpose" *Proceeding of The International Compressor Engineering Conference at Purdue.* West Lafayette, Indiana, U.S.A., Vol. I, pp. 7-11.

Rose, J. A., 1994, "*The Experimental Characterization of the Dynamics of a Reciprocating Freon Compressor System*" M.Sc. Thesis, Virginia Polytechnic Institute and State University, Mechanical Eng. Department, Blacksburg, VA, U.S.A.